Check for updates

Aerogels for the separation of asphalt-containing oil–water mixtures and the effect of asphalt stabilizer

Bin Lin, [ab] Zufei Wang, [ab] Qing-jun Zhu, [ab] Wafaa Nazurah Binti Hamzah, [c] Zhen Yao [ID] *[b] and Kun Cao [ID] *[ab]

In order to separate the asphalt-containing oil–water mixture, an aerogel film was produced through supercritical drying of a polymer gel synthesized using the ring opening metathesis polymerization of dicyclopentadiene (DCPD). The polydicyclopentadiene (PDCPD)-based aerogels have a porous structure, super-lipophilicity and super-hydrophobicity which resulted in successful separation of the simple oil–water mixture, oil–water emulsion and asphalt-containing toluene–water mixture. However, the presence of asphalt decreases the separation efficiency by blocking the pores and acting as an emulsifier. An asphalt stabilizer was then employed to reduce the asphalt particle size and weaken the flow passage blockage, consequently improving the filtration speed and the asphalt content in the filtrate. The combination of PDCPD aerogel film with an asphalt stabilizer has great application prospects for separating asphalt-containing oil–water mixtures.

1 Introduction

With the increasing amount of oil-containing wastewater in the textile, steel, food, petroleum, tanning and other industries, oil–water separation technology has become a key means to global environmental protection and waste water treatment.[1–3] In addition, frequent oil spills such as the Deepwater Horizon oil spill and the Gulf of Mexico oil spill have leaked millions of tons of crude oil into the oceans and rivers which is not only a huge threat to the environmental system but also a waste of valuable resources.[4–6] Oil spills contain chemical components such as polycyclic aromatic hydrocarbons which can persist in the water and cause chronic health effects for aquatic species such as molluscs and plants as well as compromising the thermal insulation and buoyancy of birds and mammals, all of which may only appear months or years later.[7] In the process of fuel transportation, ensuring the purity of fuel is of great significance because oil containing a small amount of water will cause serious consequences.[8] Therefore, research techniques on how to quickly and efficiently separate oil–water mixtures have received extensive attention.

Filtration and adsorption are one of the most commonly used methods for oil–water separation and have been widely used in practical industries.[9–13] Porous materials with special

wettability are commonly used in these processes.[14–18] Aerogel is a special porous material with excellent physical and chemical properties such as low density, high porosity, high surface area and adjustable surface chemistry.[19–23] In the field of oil–water separation, aerogels have a wide range of applications in adsorption and filtration.[24–28] Li *et al.*[29] prepared a polyurethane aerogel covered with graphene oxide. The aerogel has an absorption capacity for an organic solution ranging from 80 to 160 g g^{-1} and can be recycled by simple compression to remove the absorbed solvent. Inspired by the lotus leaf structure, Nguyen *et al.*[30] combined the micro/nano structure of hydrophobic graphene nanomaterials with the microporous structure of aerogel to form a rough surface, which will make the aerogel moist. The wetness changed from super-hydrophilic (water contact angle 0°) to super-hydrophobic (water contact angle 162°) while maintaining its super-lipophilicity. This graphite-based aerogel absorbs large amounts of oils and organic solvents with high selectivity, good recyclability, light weight and excellent absorption capacity of 165 g g^{-1}. Liu *et al.*[31] produced a stable cellulose/chitosan (CE/CS) aerogel with super-hydrophilic (water contact angle close to 0°) and underwater super-oleophobic (contact angle greater than 150°) by a simple method. CE/CS aerogels are effective in separating free oil–water mixtures and oil–water emulsions and still have strong separation capabilities after multiple cycles. Chen *et al.*[32] prepared a super hydrophobic TiO$_2$ (titanium oxide) nanoparticles coated cellulose aerogel with a super hydrophobic coating and a binder. The aerogel exhibits excellent super hydrophobicity (contact angle 171°) and super lipophilicity (contact angle 0°), which can separate various oil–water

[a]State Key Laboratory of Chemical Engineering, College of Chemical and Biological Engineering, Zhejiang University, Hangzhou 310027, China

[b]Institute of Polymerization and Polymer Engineering, Zhejiang University, Hangzhou 310027, China. E-mail: yaozhen@zju.edu.cn

[c]Environmental and Life Sciences, Faculty of Science, University of Brunei Darussalam, Brunei Darussalam

mixtures including chloroform, toluene, kerosene and other contaminants. Moreover, the aerogel exhibits excellent chemical and mechanical wear resistance in a variety of corrosive oil–water mixtures (such as strong acid, alkaline solution and brine environment) and alumina sandpaper.

However, in the oil–water separation process, the super-lipophilic film is easily contaminated or even clogged by the adhered or adsorbed oil or other organic particles due to their inherent lipophilicity which results in a rapid decrease influx, separation efficiency and membrane life. In addition, more waste water could be generated by subsequent cleaning of these hard-to-remove adhering or adsorbed oils.[33–35] Cao et al.[45] have prepared superhydrophobic polyurethane sponge functionalized with per-fluorinated graphene oxide, which can efficiently separate oil–water mixtures. However, the separation rate decreases greatly when filtering crude oil and water mixtures. In addition, it has been reported that the viscosity of the crude oils is the main factor affecting their absorption onto the aerogel.[46] The increase in asphalt content is also one of the main reasons for the increase in crude oil viscosity. Moreover, de Araujo et al.'s research[47] shows that asphalt can spontaneously emulsify oil–water mixtures to form a large number of emulsion droplets, which can also cause difficulties in oil–water separation. Therefore, it is of great significance to study the influence of asphalt on oil–water separation.

Dicyclopentadiene (DCPD) is a cheap by-product of the petroleum industry. The polydicyclopentadiene (PDCPD) material obtained by ring-opening metathesis polymerization (ROMP) of dicyclopentadiene monomer has gradually developed into a new type of engineering plastic due to its excellent mechanical properties and low cost.[36–38] PDCPD aerogel has the advantages of a wide range of raw materials, low cost, easy preparation, low density, high porosity, and excellent physical and chemical properties,[39,40] which makes it an ideal choice for oil–water separation materials. In this paper, a PDCPD-based aerogel film was prepared from PDCPD gel by supercritical drying process, and used for separation of the simple oil–water mixture, oil–water emulsion and asphalt-containing toluene–water mixture. The effects of asphalt, a common component in crude oil and its stabilizer had been investigated.

2 Experimental

2.1 Materials

Dicyclopentadiene was provided by TCI (Shanghai) Chemical Industry Development Co., Ltd. for the synthesis of poly-dicyclopentadiene. The first generation Grubbs catalyst was purchased from Saen Chemical Technology (Shanghai) Co., Ltd. The toluene and acetone were obtained from Jiangsu Yonghua Fine Chemicals Co., Ltd. and China National Chemicals Co., Ltd., respectively. Emulsifier, Span80, was supplied by J&K Scientific Ltd. Asphalene stabilizer, SNODMI (poly(styrene-alt-octadecyl maleimide)), was synthesized in our laboratory.[41]

2.2 Preparation of PDCPD aerogel

PDCPD aerogel was prepared according to the adapted method.[39,40] The aerogel preparation process are shown in

Fig. 1. The DCPD was distilled off under reduced pressure to remove the polymerization inhibitor, and the calcined molecular sieve was added to remove residual moisture. In the synthesis process, the Grubbs catalyst was added to a DCPD/toluene solution. After 90 s, the reaction liquid was transferred to an evaporating dish to form a film of 0.25 cm thick. After standing for 24 hours, the aged wet gel was transferred to toluene whose volume was 4 times that of the gel. The toluene was changed every 8 hours for a total of three replacements. The wet gel was then transferred to a beaker filled with acetone which was changed every 8 hours for a total of three changes. After the acetone replacement, the wet gel went through a supercritical drying process which includes batch liquid carbon dioxide displacement, continuous liquid carbon dioxide displacement and supercritical drying to finally obtain a corresponding aerogel.

Fig. 2 shows the infrared results for DCPD and PDCPD-aerogels. In the DCPD infrared spectrum, the absorption peak at 1571 cm^{-1} is assigned to the C=C stretching vibration on the norbornene ring. The absorption peak at 1614 cm^{-1} belongs to the C=C stretching vibration on the cyclopentene ring. On the PDCPD absorption curve, the absorption peak at 1571 cm^{-1} disappeared. A new absorption peak appeared at 1704 cm^{-1}, which is a C=C stretching vibration peak on the acyclic olefin. The C=C stretching vibration absorption peak on the cyclopentene ring still remains and migrates from 1614 cm^{-1} to 1620 cm^{-1}.

2.3 Preparation of different oil–water mixtures

Oil–water mixture: 30 mL of toluene(or chloroform, n-decane), 70 mL of deionized water and a small amount of coloring agent (Sudan III) were mixed and stirred for one hour.

Oil–water emulsion: 30 mL of toluene, 70 mL of deionized water and 0.5 mL of Span80 were mixed and stirred for three hours to obtain a stable emulsion.

Asphalt-containing oil–water mixture: 0.783 g of asphalt was dissolved in 30 mL of toluene to prepare a 3 wt% asphalt/
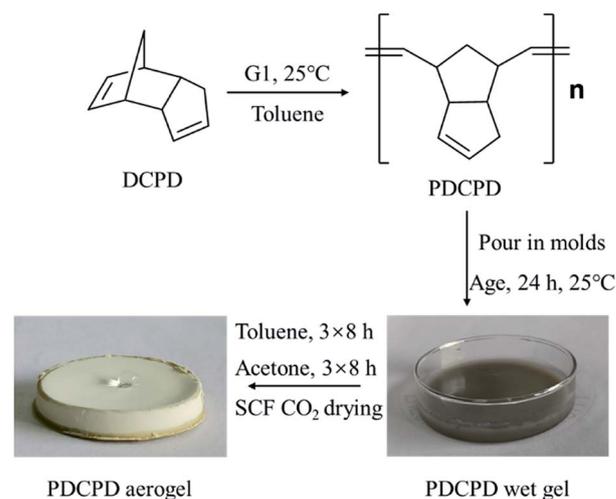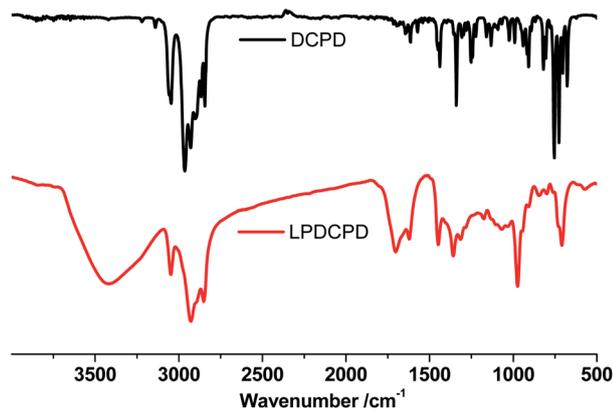

Fig. 1 Preparation of PDCPD aerogel.

Fig. 2 FTIR spectrum of DCPD and PDCPD.

toluene solution. 70 mL of deionized water was added to prepare an asphalt-containing oil–water mixture without SNODMI.

The asphalt-containing oil–water mixture with SNODMI: 0.054 g of SNODMI was dissolved in 30 mL of toluene followed by addition of 0.783 g asphalt. After the dissolution was completed, 70 mL of deionized water was added.

2.4 Oil–water separation experiment

The aerogel film was used as a filter membrane inserted in between the suction devices. The pressure difference between the outlet pressure of the vacuum pump and the atmospheric pressure was controlled at 300 mbar. The filtration time was started after pouring the oil–water mixture. After completion of the filtration, the filtrate phase and the aqueous phase of which did not pass through the aerogel film were obtained.

2.5 Characterization method

ThermoFisher's Nicolet 5700 infrared spectrometer was used for structural analysis. The detector used was DTGS KBr with a scanning wavenumber range of 400–4000 cm^{-1} and a resolution of 0.1 cm^{-1}. The OCA 20 video optical contact angle measuring instrument from Data physics of Germany was used to measure the water contact angle of aerogels surface. The SEM test was performed on a field emission scanning electron microscope Hitachi SU 8010. The water content in the filtrate was determined by a C20 trace moisture meter from Mettler Toledo.

3 Results and discussion

3.1 Synthesis of aerogels

PDCPD was synthesized using the first-generation Grubbs catalysts. Gels with three different polymer mass concentrations 6 wt%, 8 wt% and 12 wt% were prepared and the corresponding aerogel samples are named P6, P8 and P12 respectively.

Wettability is important for oil–water separation materials. Fig. 3a shows the water contact angle test results of PDCPD aerogel, where the water contact angles of P6, P8 and P12 are

127°, 128° and 131° respectively. In the literature reported so far, the water contact angle range of common hydrophobic aerogels is generally between 114–171°.[30,32,42] The PDCPD aerogels prepared here are at a moderate level. Seen from Fig. 3b, water droplets stained with methylene blue cannot on the other hand, Fig. 3c shows that toluene droplets stained with Sudan III are rapidly absorbed by the aerogel. Therefore, PDCPD aerogels exhibit hydrophobicity and lipophilicity.

3.2 Analysis of SEM results of aerogels

Fig. 4 illustrates the morphology of PDCPD aerogels with magnifications of 1000 and 10 000. It can be found that the PDCPD aerogels are composed of cellulose-like aggregates that are interconnected to form open-cell structures of different sizes and shapes. DCPD was polymerized under the action of first generation Grubbs catalyst to form macromolecules which interacted with the solvent to form a gel. In the supercritical drying process, the original liquid solvent was replaced with supercritical carbon dioxide and finally the porous structure was formed after releasing CO_2. Comparing the SEM images of the samples P6, P8 and P12, it can be seen that the aerogel pore structure after drying is denser and the pore diameter is smaller as the concentration of the wet gel was increased.

3.3 Separation of simple oil–water mixtures

PDCPD aerogel can be used for oil–water separation due to its hydrophobicity, lipophilicity and porous structure. As shown in Fig. 5a, toluene containing methyl orange dyed can pass through the aerogel film but water cannot pass which then leads to the formation of a toluene filtrate phase (left side of Fig. 5b) and an aqueous phase (right side of Fig. 5b). In the separation experiment using the sample P8 as a filtration membrane, the water content in the toluene filtrate was reduced to 196.7 ppm in the oil–water mixture, and the filtration rate was 3.46 L h^{-1} m^{-2} kPa^{-1}.

In order to investigate the separation performance of PDCPD aerogel membranes for other organic liquid and water mixtures, PDCPD aerogel membranes were applied to separate chloroform–water mixtures and n-decane–water mixtures. The results are shown in Fig. 6 and 7, respectively. Organic liquids can successfully pass through the PDCPD aerogel membrane, while
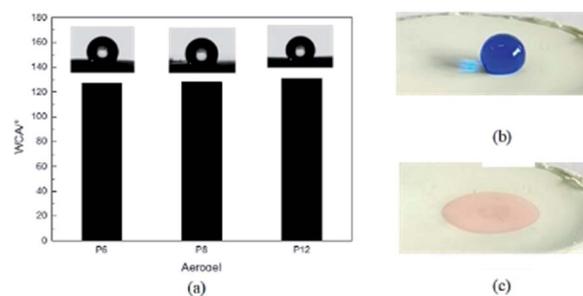

Fig. 3 Wettability of aerogel: (a) the water contact angle of aerogels; (b) the water droplet on the surface of the aerogel & (c) the toluene droplet on the surface of the aerogel.
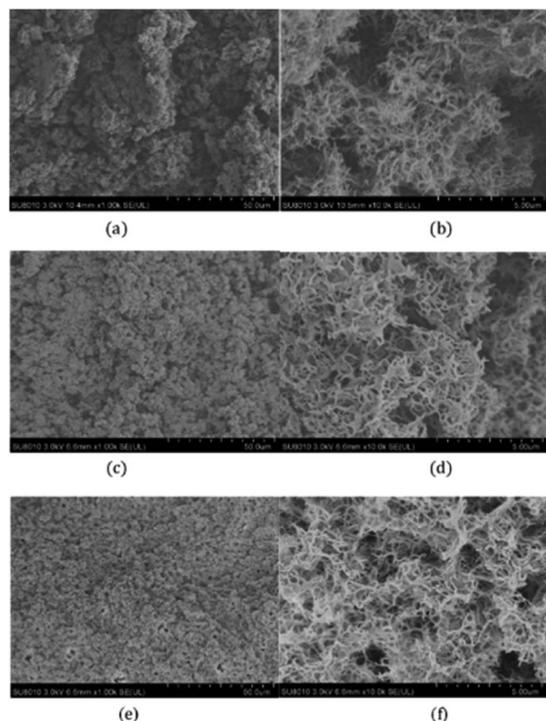
Fig. 4 SEM for PDCPD-based aerogels: P6: (a and b); P8: (c and d) & P12: (e and f).

water cannot. As a result, the aerogel membrane successfully separated the oil–water mixture, and the passing rates of chloroform and n-decane were 2.99 L h^{-1} m^{-2} kPa^{-1} and 2.81 L h^{-1} m^{-2} kPa^{-1}, respectively.

3.4 Separation of oil–water emulsion

The oil–water emulsion is more difficult to separate because of its stable emulsion structure. In this study, a stable emulsion was prepared by using Span 80 emulsifier and the separation effect of PDCPD aerogel was investigated. As shown in Fig. 8a, only the clarified toluene in the oil–water emulsion can pass through the
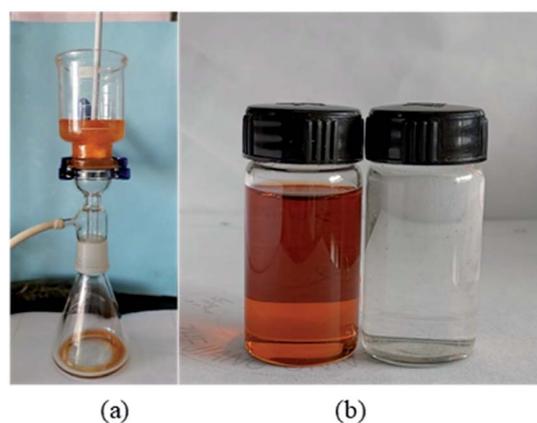

Fig. 5 Separation of toluene–water mixtures with PDCPD aerogel: (a) experimental setup; (b) filtrate phase (left) and residual phase (right).
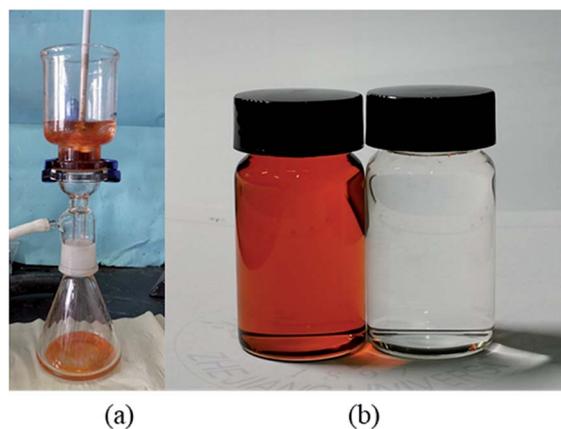

Fig. 6 Separation of chloroform–water mixtures with PDCPD aerogel: (a) experimental setup; (b) filtrate phase (left) and residual phase (right).

aerogel. The filtration results are shown in Fig. 8b. The left side is the pre-filtration emulsion and the right side is the filtered clear liquid. The water content was reduced to 348.7 ppm in the toluene filtrate. The filtration rate was 0.798 L h^{-1} m^{-2} kPa^{-1} which is much lower than the simple oil–water separation because the emulsion separation requires a greater driving force and the emulsifier blocks the filtration channel to some extent.

3.5 Separation of oil–water mixture with asphalt

In order to investigate the effect of asphalt on oil–water separation, a 3 wt% asphalt–toluene solution was prepared in this study. The oil–water mixture was prepared according to the volume ratio of toluene : water = 3 : 7. The oil–water mixture with asphalt was subjected to filtration experiments using P6, P8 and P12 respectively. An asphalt stabilizer, SNODMI, was added to the 3 wt% asphalt–toluene solution to investigate the effect of asphalt stabilizers on the separation of asphalt-containing oil–water mixtures.
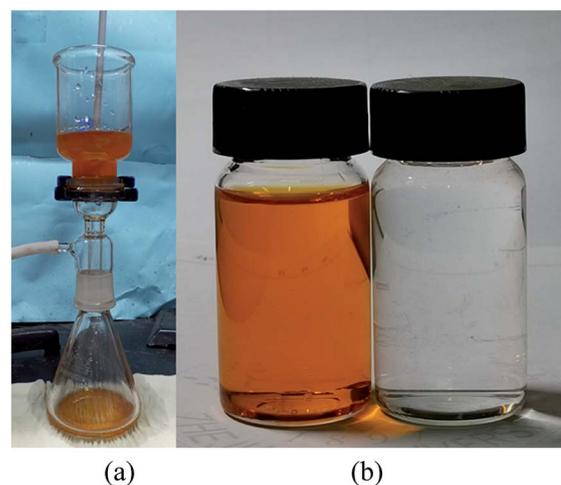

Fig. 7 Separation of n-decane–water mixtures with PDCPD aerogel: (a) experimental setup; (b) filtrate phase (left) and residual phase (right).
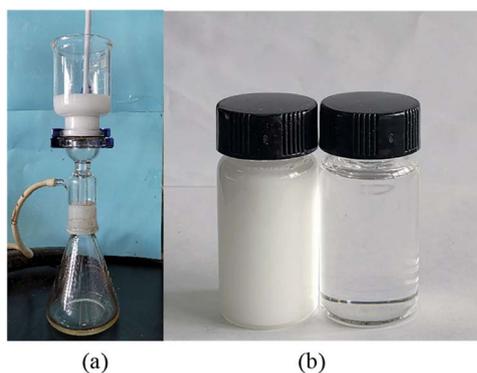
Fig. 8 Separation of oil–water emulsion with PDCPD aerogel: (a) experimental setup; (b) residual phase (left) and filtrate phase (right).

Fig. 10 Effects of SNODMI on filtration speed of asphalt-containing oil–water mixture separation process.

As shown in Fig. 9a, the asphalt-containing toluene can pass through the PDCPD aerogel film but the water cannot pass through the hydrophobic aerogel film which results in the formation of the filtrate phase as shown in Fig. 9b (left) and the water phase (right). It can be concluded that the aerogel film can effectively separate the asphalt-containing oil–water mixtures.

The effects of SNODMI on the filtration rate are shown in Fig. 10 for various PDCPD aerogel film. It can be seen that the filtration speed for the asphalt oil–water mixture without SNODMI is similar to that of the emulsion separation and that is much lower than $3.46 \text{ L h}^{-1} \text{ m}^{-2} \text{ kPa}^{-1}$ (the filtration speed of simple oil–water mixture). This is caused by the following reasons: (1) the asphalt can play a role of emulsifier in the oil–water mixture,[43,44] hence the driving force required for filtration after forming the emulsion increases resulting in a decrease in the filtration speed. (2) The asphalt particles adhered to the fibrous structure of the aerogel when it was filtered. When the asphalt concentration is high, the pores will be blocked to a certain extent which reduces the passage of toluene through the aerogel film. With the addition of the asphalt stabilizer SNODMI, the filtration speed using P6 and P8 were greatly increased while the effect on the filtration speed using P12 was insignificant. The same trend was also observed when the
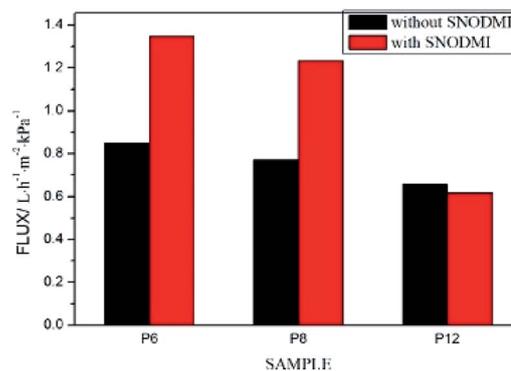
effects of the asphalt stabilizer on the asphalt content of the filtrate were investigated. For the P6 and P8 samples, the asphalt content in the filtrate was greatly increased after adding SNODMI. This may be because the asphalt stabilizer can stabilize the asphalt particles below a certain particle size. The pore size of the P6 and P8 aerogel is large enough that a large amount of asphalt particles can pass through the aerogel film. Since the asphalt stabilizer can reduce the amount of asphalt particles attached to the surface of the aerogel film, thereby simultaneously increasing the filtration speed and the total amount of the asphalt in the filtrate with relatively larger pore size, the improvement effect of SNDOMI is more significant. In comparison to the P12 aerogel with the smallest pore size, the flow passage can be easily blocked by the asphalt particles. Although SNODMI can reduce the average diameter of the asphalt particles in the oil–water mixture, they were not small enough and have little effect on the filtration process (Fig. 11).

In order to verify the effect of asphalt on oil–water separation, the morphologies of the aerogel membranes before and after filtration were observed using SEM. Fig. 12(a and b) present the SEM image of P6 film before filtration. The SEM image of P6 film after separation of asphalt-containing oil–water mixture without SNODMI are shown in Fig. 12(c and d). The SEM image after adding SNODMI are illustrated in Fig. 12(e
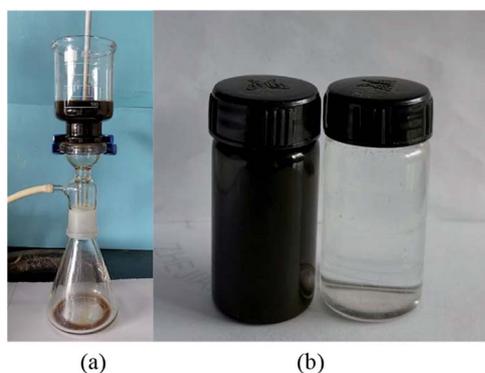

Fig. 9 Separation of asphalt-containing oil–water mixtures with PDCPD aerogel: (a) experimental setup; (b) filtrate phase (left) and residual phase (right).
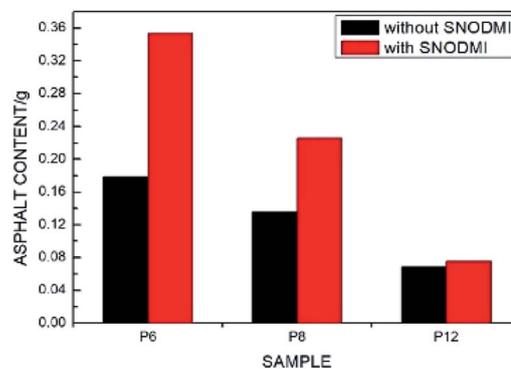

Fig. 11 Effects of SNODMI on the asphalt content in the filtrate phase of asphalt-containing oil–water mixture separation process.
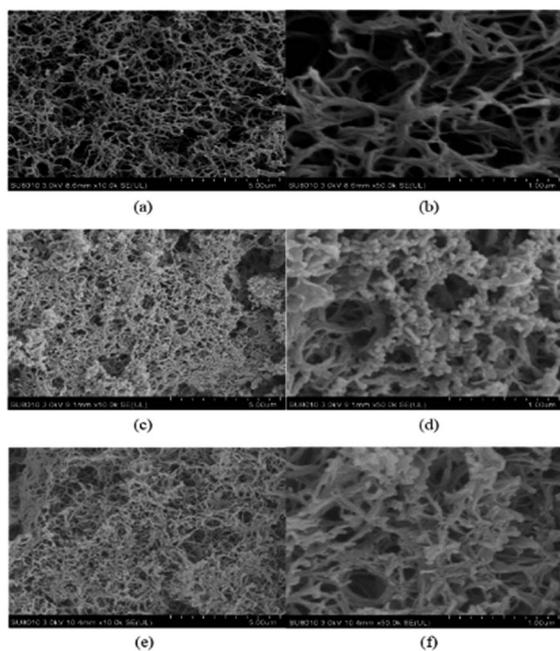
Fig. 12 SEM images of aerogel P6: (a and b): before filtration; (c and d): after filtration of asphalt-containing oil–water mixture without SNODMI; (e and f): after filtration of asphalt-containing oil–water mixture with SNODMI.

and f). It can be seen from the figure that, a large amount of asphalt particles were precipitated on the wall of the pore and blocked the passage of toluene after the separation process. With the addition of SNODMI, the amount of asphalt particles attached to the pore structure was significantly reduced and more opening were available for toluene to pass through.

4   Conclusions

In this research, PDCPD gel was synthesized by ring-opening metathesis polymerization using the first generation first-generation Grubbs catalyst. After solvent replacement and supercritical drying of the PDCPD gel, an aerogel film with super-lipophilic and super-hydrophobic behaviors were obtained. The simple oil–water mixture, oil–water emulsion and asphalt-containing toluene–water mixture have been successfully separated using the PDCPD-aerogel film. The asphalt deteriorates the separation efficiency by blocking the pores and acting as an emulsifier. After adding the asphalt stabilizer SNODMI, the asphalt particle size was reduced. When aerogel films with relatively large pore size were used, the flow passage blockage was alleviated resulting in increased the filtration speed and the asphalt content in the filtrate. Therefore, PDCPD aerogel and asphalt stabilizer SNODMI are promising combination for separating asphalt-containing oil–water mixture.

Conflicts of interest

There are no conflicts to declare.

Acknowledgements

References

1   L. P. Gossen and L. M. Velichkina, *Pet. Chem.*, 2006, **46**, 67–72.
2   D. Mysore, T. Viraraghavan and Y. C. Jin, *J. Residuals Sci. Technol.*, 2006, **3**, 5–14.
3   M. Padaki, R. S. Murali, M. S. Abdullah, N. Misdan, A. Moslehyani, M. A. Kassim, N. Hilal and A. F. Ismail, *Desalination*, 2015, **357**, 197–207.
4   A. B. Nordvik, J. L. Simmons, K. R. Bitting, A. Lewis and T. StromKristiansen, *Spill Sci. Technol. Bull.*, 1996, **3**, 107–122.
5   M. O. Adebajo, R. L. Frost, J. T. Kloprogge, O. Carmody and S. Kokot, *J. Porous Mater.*, 2003, **10**, 159–170.
6   M. Kammerer, O. Mastain, S. Le Deran-Quenech'du, H. Pouliquen and M. Larhantec, *Sci. Total Environ.*, 2004, **333**, 295–301.
7   S. Ngene, K. Tota-Maharaj, P. Eke and C. Hills, *International Journal of Economy, Energy and Environment*, 2016, **1**, 64–73.
8   W. F. Zhang, N. Liu, Y. Z. Cao, X. Lin, Y. N. Liu and L. Feng, *Adv. Mater. Interfaces*, 2017, **4**, 1600029.
9   B. Van der Bruggen, C. Vandecasteele, T. Van Gestel, W. Doyen and R. Leysen, *Environ. Prog.*, 2003, **22**, 46–56.
10 G. M. Geise, H. S. Lee, D. J. Miller, B. D. Freeman, J. E. Mcgrath and D. R. Paul, *J. Polym. Sci., Part B: Polym. Phys.*, 2010, **48**, 1685–1718.
11 R. K. Gupta, G. J. Dunderdale, M. W. England and A. Hozumi, *J. Mater. Chem. A*, 2017, **5**, 16025–16058.
12 G. H. Meng, H. L. Peng, J. N. Wu, Y. X. Wang, H. Wang, Z. Y. Liu and X. H. Guo, *Fibers Polym.*, 2017, **18**, 706–712.
13 G. F. Li, X. Wang, L. Tao, Y. S. Li, K. C. Quan, Y. Wei, L. F. Chi and Q. P. Yuan, *J. Membr. Sci.*, 2015, **495**, 439–444.
14 B. Wang, W. X. Liang, Z. G. Guo and W. M. Liu, *Chem. Soc. Rev.*, 2015, **44**, 336–361.
15 Q. L. Ma, H. F. Cheng, A. G. Fane, R. Wang and H. Zhang, *Small*, 2016, **12**, 2186–2202.
16 C. Ao, R. Hu, J. Zhao, X. Zhang, Q. Li, T. Xia, W. Zhang and C. Lu, *Chem. Eng. J.*, 2018, **338**, 271–277.
17 X. Yang, J. Ma, J. Ling, N. Li, D. Wang, F. Yue and S. Xu, *Appl. Surf. Sci.*, 2018, **435**, 609–616.
18 X. J. Yue, T. Zhang, D. Y. Yang, F. X. Qiu and Z. D. Li, *J. Cleaner Prod.*, 2018, **199**, 411–419.
19 L. X. Li, B. C. Li, H. X. Sun and J. P. Zhang, *J. Mater. Chem. A*, 2017, **5**, 14858–14864.
20 F. Deuber, S. Mousavi, L. Federer and C. Adlhart, *Adv. Mater. Interfaces*, 2017, **4**, 1700065.
21 J. Q. Wan, J. M. Zhang, J. Yu and J. Zhang, *ACS Appl. Mater. Interfaces*, 2017, **9**, 24591–24599.
22 Y. F. Tang, Q. F. Zheng, B. Chen, Z. Q. Ma and S. Q. Gong, *Nano Energy*, 2017, **38**, 401–411.

23 W. C. Wan, R. Y. Zhang, W. Li, H. Liu, Y. H. Lin, L. N. Li and Y. Zhou, *Environ. Sci.: Nano*, 2016, **3**, 107–113.

24 R. Li, C. B. Chen, J. Li, L. M. Xu, G. Y. Xiao and D. Y. Yan, *J. Mater. Chem. A*, 2014, **2**, 3057–3064.

25 J. H. Li, J. Y. Li, H. Meng, S. Y. Xie, B. W. Zhang, L. F. Li, H. J. Ma, J. Y. Zhang and M. Yu, *J. Mater. Chem. A*, 2014, **2**, 2934–2941.

26 X. C. Dong, J. Chen, Y. W. Ma, J. Wang, M. B. Chan-Park, X. M. Liu, L. H. Wang, W. Huang and P. Chen, *Chem. Commun.*, 2012, **48**, 10660–10662.

27 Y. Du, Y. Li and T. Wu, *RSC Adv.*, 2017, **7**, 41838–41846.

28 Z. He, X. Zhang and W. Batchelor, *RSC Adv.*, 2016, **6**, 21435–21438.

29 Y. Liu, J. K. Ma, T. Wu, X. R. Wang, G. B. Huang, Y. Liu, H. X. Qiu, Y. Li, W. Wang and J. P. Gao, *ACS Appl. Mater. Interfaces*, 2013, **5**, 10018–10026.

30 D. D. Nguyen, N. H. Tai, S. B. Lee and W. S. Kuo, *Energy Environ. Sci.*, 2012, **5**, 7908–7912.

31 H. Peng, J. Wu, Y. Wang, H. Wang, Z. Liu, Y. Shi and X. Guo, *Appl. Phys. A*, 2016, **122**.

32 H. Zhang, Y. Q. Li, Z. X. Lu, L. H. Chen, L. L. Huang and M. Z. Fan, *Sci. Rep.*, 2017, **7**, 9428.

33 Y. Q. Du, Y. J. Li and T. Wu, *RSC Adv.*, 2017, **7**, 41838–41846.

34 Z. X. Xue, S. T. Wang, L. Lin, L. Chen, M. J. Liu, L. Feng and L. Jiang, *Adv. Mater.*, 2011, **23**, 4270–4273.

35 Q. F. Wei, R. R. Mather, A. F. Fotheringham and R. D. Yang, *Mar. Pollut. Bull.*, 2003, **46**, 780–783.

36 Z. Yao, L. W. Zhou, B. B. Dai and K. Cao, *J. Appl. Polym. Sci.*, 2012, **125**, 2489–2493.

37 K. Cao, Q. Fu, L. Zhou and Z. Yao, *Prog. Chem.*, 2012, **24**, 1368–1377.

38 F. Hu and Y. Zheng, *Polym. Bull.*, 2011, 139–150.

39 A. Bang, D. Mohite, A. M. Saeed, N. Leventis and C. Sotiriou-Leventis, *J. Sol-Gel Sci. Technol.*, 2015, **75**, 460–474.

40 J. K. Lee and G. L. Gould, *J. Sol-Gel Sci. Technol.*, 2007, **44**, 29–40.

41 K. Cao, Q.-j. Zhu, X.-x. Wei, Y.-f. Yu and Z. Yao, *Energy Fuels*, 2016, **30**, 2721–2728.

42 H. C. Bi, X. Xie, K. B. Yin, Y. L. Zhou, S. Wan, L. B. He, F. Xu, F. Banhart, L. T. Sun and R. S. Ruoff, *Adv. Funct. Mater.*, 2012, **22**, 4421–4425.

43 J. R. Samaniuk, E. Hermans, T. Verwijlen, V. Pauchard and J. Vermant, *J. Dispersion Sci. Technol.*, 2015, **36**, 1444–1451.

44 H. W. Yarranton, H. Hussein and J. H. Masliyah, *J. Colloid Interface Sci.*, 2000, **228**, 52–63.

45 N. Cao, J. Y. Guo, R. Boukherroub, Q. G. Shao, X. B. Zang, J. Li, X. Q. Lin, H. Ju, E. Y. Liu, C. F. Zhou and H. P. Li, *Sci. China: Technol. Sci.*, 2019, **62**, 1585–1595.

46 S. T. Nguyen, J. D. Feng, N. T. Le, N. Hoang, V. B. C. Tan and H. M. Duong, *Ind. Eng. Chem. Res.*, 2013, **52**, 18386–18391.

47 S. B. de Araujo, M. Merola, D. Vlassopoulos and G. G. Fuller, *Langmuir*, 2017, **33**, 10501–10510.